

Thermal and electronic properties of rare-earth $\text{Ba}_2\text{Cu}_3\text{O}_x$ superconductors

J. Heremans, D. T. Morelli, G. W. Smith, and S. C. Strite III*

Physics Department, General Motors Research Laboratories, Warren, Michigan 48090-9055

(Received 27 October 1987)

We have measured the electrical resistivity, thermal conductivity, and specific heat of a series of high-temperature superconducting compounds of the form $R\text{Ba}_2\text{Cu}_3\text{O}_7$, with $R = \text{Y, Eu, Gd, Dy, and Er}$. Our results show that the aforementioned physical properties are virtually identical for all samples considered. In particular, the molar specific heats are identical to within $\pm 2\%$ and exhibit Debye-type behavior. We observe a nearly constant thermal conductivity above T_c , but a rather sudden increase develops as the temperature is lowered below the critical temperature. The electrical resistivity is nearly linear in the normal state. Thermal and electrical conductivities indicate that for $T > T_c$, the predominant electron scattering mechanism is due to phonon interactions. Using the electrical resistivity data and the Wiedemann-Franz law, we estimate the magnitude of the electronic component of the thermal conductivity to be an order of magnitude smaller than the measured thermal conductivity. We thus conclude that heat transport is predominantly by phonons. The enhancement of the lattice conduction below the critical temperature is understood as a reduction of carrier-phonon scattering as electrons condense into Cooper pairs. This lends support to standard Bardeen-Cooper-Schrieffer-type phonon-mediated superconductivity. An estimate of the superconducting transition temperatures is made using the electron-phonon coupling constants and Debye temperatures deduced from the data which bracket the observed T_c quite well. We discuss the thermal conductivity at very low temperature in terms of a phonon mean-free path limited by pores in the samples.

INTRODUCTION

The exciting technological promise of the new high-temperature superconductors has given birth to a gigantic effort in investigating, both experimentally and theoretically, their properties. While a wealth of data already exists on the composition dependence, critical fields, energy gap, structure, etc., of these compounds, a clear picture of what mechanism is responsible for their high transition temperatures has not yet been formed. Central to this question is whether these materials are standard Bardeen-Cooper-Schrieffer (BCS)-type superconductors, i.e., whether the electron-phonon interaction is large enough to support the high transition temperatures observed to date. Early indications, based on the apparent absence of a copper or barium isotope effect¹ and the non-saturation of the high-temperature resistivity,² suggest the existence of a carrier coupling mechanism not due to the lattice alone. Recent observations of a small oxygen isotope effect,³ on the other hand, lend support to a BCS-type explanation for superconductivity in these compounds. Thus it is safe to say that the question of the mechanism governing superconduction in these systems is still up in the air.

One of the most useful probes for determining interactions between carriers and phonons is the thermal conductivity. In a recent report,⁴ we showed that phonons are indeed scattered strongly by electrons in Y-Ba-Cu-O, and that the scattering decreased significantly when the carriers condensed into superconducting pairs. This observation has recently been confirmed by others.⁵ An interest-

ing question is whether this interaction is changed in any way by the substitution of a rare-earth element for yttrium in the lattice. Here we report our observations of the electrical resistivity, thermal conductivity, and specific heat of a series of rare-earth barium-copper-oxygen superconductors, and we present quantitative information on the strength of the electron-phonon coupling and how it depends on the composition of the material.

EXPERIMENT

Samples were fabricated according to the standard recipes, the details of which we have presented in an earlier report.⁴ The integrity of the resulting material was investigated using both chemical and x-ray analysis. In Table I the composition of each sample is presented, and Fig. 1 shows an x-ray diffractogram of each sample as well as an x-ray spectrum calculated from the expected atomic positions.⁶ The conclusion is that, with the possible exception of the Er-based compound, our samples are at least 90% 1:2:3 phase.

The transport properties were measured using a closed-cycle helium-4 cryostat capable of reaching 8 K. Thermal conductivity data on one yttrium-based sample were taken down to 2 K using a liquid-helium cryostat. The heat-capacity measurements were performed on a Perkin-Elmer model DSC-2 differential scanning calorimeter (DSC) in the temperature range 240–490 K. The type of measurement being performed determined the geometry of the sample. For electrical resistivity measurements,

TABLE I. Measured parameters of $RBa_xCu_yO_7$. R represents the rare-earth component, x the barium fraction, y copper fraction. ρ_m and ρ_e are the measured and expected mass densities, and r is the porosity. A is the impurity resistivity and B the temperature coefficient of resistivity; κ ($T > T_c$) is the measured thermal conductivity above the transition temperature.

R	x	y	T_0 (K)	ρ_m ($g\ cm^{-3}$)	ρ_e ($g\ cm^{-3}$)	r	A ($m\ \Omega\ cm$)	B ($\mu\ \Omega\ cm\ K^{-1}$)	κ ($T > T_c$) ($W\ cm^{-1}\ K$)
Gd	1.98	3.05	89.4	3.83	7.02	0.46	3.7	8.0	0.0053
Dy	1.97	3.06	87.1	4.48	7.07	0.37	4.2	7.8	0.0083
Eu	1.93	2.92	83.2	3.69	6.97	0.47	8.0	7.4	0.0085
Y	2.01	3.11	86.0	2.72	6.37	0.57	7.6	39.0	0.0052
Er	2.03	3.05	90.0	3.01	7.12	0.58	15.3	26.0	0.0054

samples were cut from a pressed disk into parallelepipeds of approximate dimensions $1 \times 2 \times 15\ mm^3$. These were glued over an insulating layer of cigarette paper onto the cold head using GE 7031 varnish. Current and voltage probes were 40 gauge copper wires attached with a small drop of silver paint. In order to ensure Ohmic behavior of the contacts, the measuring current was varied between 1 and 100 mA, with only a few percent change in the resistance. The current was then fixed at 10 mA for the remaining measurements. The cold-tip temperature was controlled using a Lakeshore model 520 temperature con-

troller in conjunction with calibrated platinum and carbon-glass thermometers.

Because the thermal conductivity of these compounds is rather small, it is advantageous, as far as heat conduction experiments are concerned, to have a rather short, fat sample in order to maximize heat conduction through the sample relative to heat losses. Thus we used samples of nominal dimensions of $3 \times 5 \times 10\ mm^3$ for thermal conductivity measurements. Details of the measuring technique are given in our earlier report.⁴ Briefly, one end of the sample was glued to the cold tip, and a small metal film heater was attached on the free end. The temperature difference across the sample as heat flowed through it was measured with a Chromel-constantan thermocouple. In the low-temperature (2–6 K) measurements, the thermocouple was replaced by a pair of calibrated germanium resistance thermometers which have an accuracy of better than 0.5 mK in this temperature range.

Each DSC sample, a rectangular slab weighing from 115 to 185 mg, was placed in a small aluminum pan which was mounted in the calorimeter sample holder; an almost identical empty aluminum pan was mounted in the DSC reference holder. The specific-heat measurement was performed by scanning the temperature at 20 K/min over the range of interest while monitoring the excess power required to maintain the sample temperature equal to that of the reference. This power curve was then corrected for differences in the thermal characteristics of the two aluminum pans by removing the sample from its pan and repeating the scan. The resulting empty pan power curve was then subtracted from the sample curve to yield a corrected differential power curve proportional to the specific heat. The proportionality constant was obtained from a determination of the melting enthalpy of indium. The accuracy of this method was verified by measuring the specific heat of sapphire; the results agreed with literature values to within 1% in our temperature range.

RESULTS

Figure 2 exhibits the resistivity of five samples as a function of temperature. We see that the resistivity is approximately linear with T down to about 120 K, at which point it begins to drop precipitously as the samples begin to superconduct. Table I shows the zero-resistance temperature (T_0) for each sample. Also shown in this table is

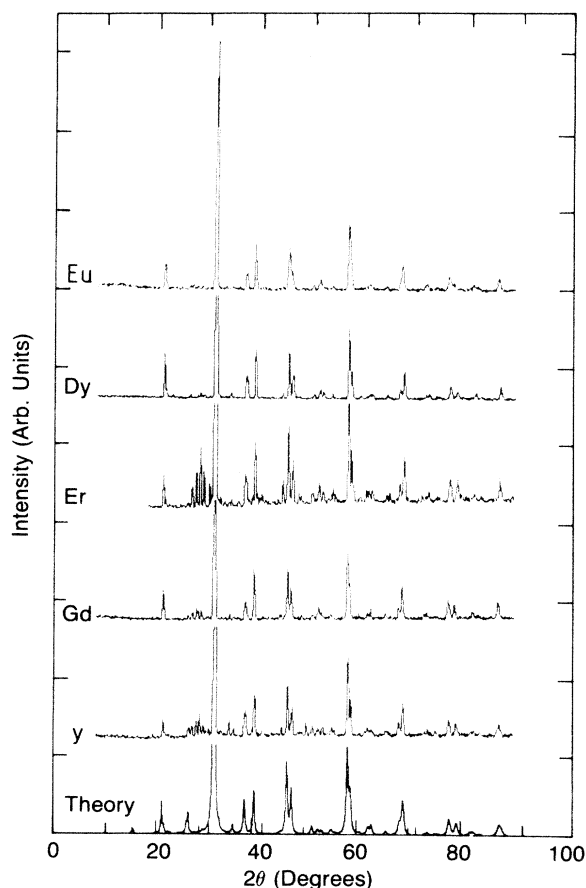


FIG. 1. Diffractometer scan of five superconducting oxides, and that calculated from atomic positions.

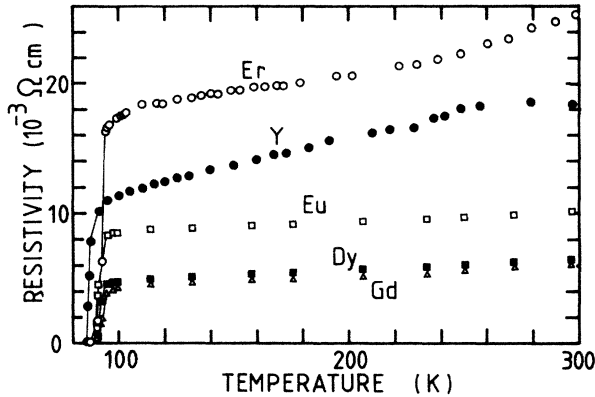


FIG. 2. Resistivity as a function of temperature for five samples studied.

the porosity, which is given by

$$r = 1 - \rho_m / \rho_e,$$

where ρ_m is the measured density of the sample and ρ_e the expected density as calculated from the unit-cell dimensions. We see from Fig. 3 that the resistivity of these materials increases with porosity. This is to be expected because a more porous sample has a smaller effective cross section through which charge carriers can pass. We will see below that the porous nature of these materials affects significantly the degree to which heat is conducted through them as well.

The linearity of the electrical resistivity above the transition temperature of each sample as well as the large magnitude of ρ suggest that charge carriers are scattered

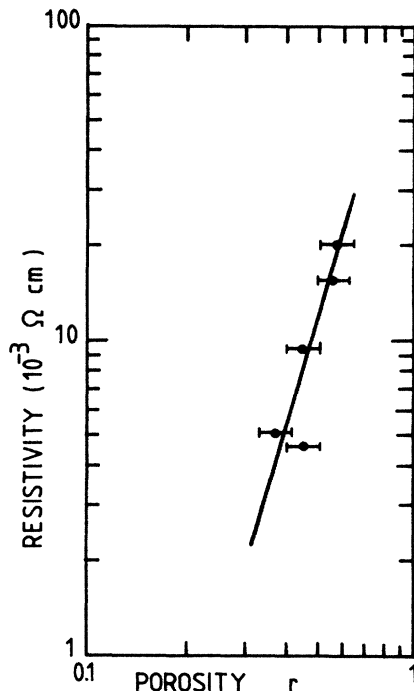


FIG. 3. Resistivity at 120 K as a function of sample porosity.

quite strongly by phonons as well as defects in this temperature range. In order to gain an estimate of the relative contributions of these to scattering mechanisms, we write the total resistivity of each sample, according to Matthiessen's rule,⁷ as

$$\rho = A + BT$$

with A a constant and $B = d\rho/dT$. The first term is the resistivity due to scattering by defects and impurities, and the linear term arises from phonon scattering. Fitting this equation to the data gives the parameters A and B listed in Table I.

Our thermal conductivity results are summarized in Fig. 4. All samples show the same general trend: At high temperature the thermal conductivity is nearly constant, but as the samples become superconducting the thermal conductivity is *enhanced* before reaching a peak near 55–60 K and falling off at lower temperature. Because these compounds are metallic, heat can be conducted by both lattice vibrations and charge carriers. In most normal metals, thermal conduction by electrons far exceeds that of phonons due to the high charge density. To gain an estimate of the magnitude of the carrier thermal conductivity κ_c in the compounds studied here, we make use of the Wiedemann-Franz law, which states that, if the scattering of charge carriers is elastic, then

$$\kappa_c \rho = L_0 T,$$

where $L_0 = (\pi^2/3)(k_B/e)^2 = 2.45 \times 10^{-8} \text{ V}^2 \text{ K}^{-2}$. If the carriers are not scattered totally elastically, this formula gives an upper limit to the carrier thermal conductivity. Our estimates of κ_c at 100 K using this formula are given in Table I, along with the actual saturation value of the thermal conductivity at high temperature ($T > T_c$). We see that the electronic component is at most only 10% of the total measured thermal conductivity, and in most

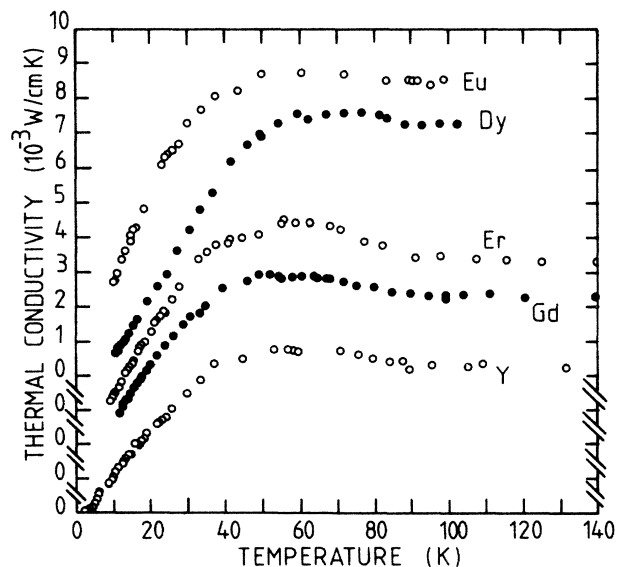


FIG. 4. Thermal conductivity vs temperature for five samples investigated. Note that the vertical axis for each sample has been displaced one unit for clarity.

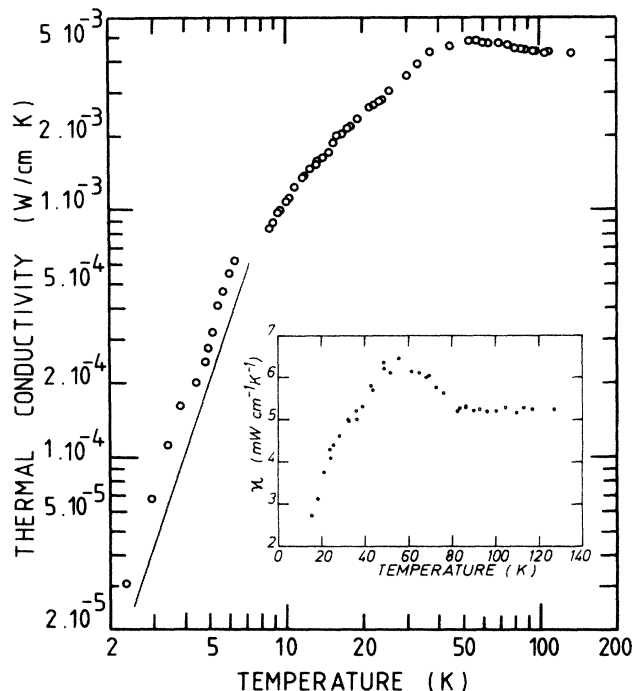


FIG. 5. Thermal conductivity vs temperature down to 2 K for $\text{YBa}_2\text{Cu}_3\text{O}_7$ sample. The bold line indicates T^3 dependence. The inset shows the data around T_c on a linear scale to emphasize the anomaly.

cases significantly less. Thus nearly all of the heat is being conducted by the lattice. The thermal conductivity well below the transition temperature for one sample of $\text{YBa}_2\text{Cu}_3\text{O}_7$ is shown in Fig. 5; we find that in this temperature regime $\kappa \sim T^3$.

Figure 6 represents the molar specific heat for all five samples in the temperature range 240–490 K. Each curve was obtained by multiplying the measured specific heat per unit mass by the formula weight, as given in Table II. The molar specific heats so obtained are found to vary by only $\pm 2\%$ between the different rare-earth constituents. Values of the Debye temperature derived from the fit of the Debye function to the specific heat are listed in Table III. The high-temperature limiting values of our fit to the Debye function, C_{00} , are compared in this table to the theoretical Dulong-Petit value $3n_i k_B$, where n_i is the num-

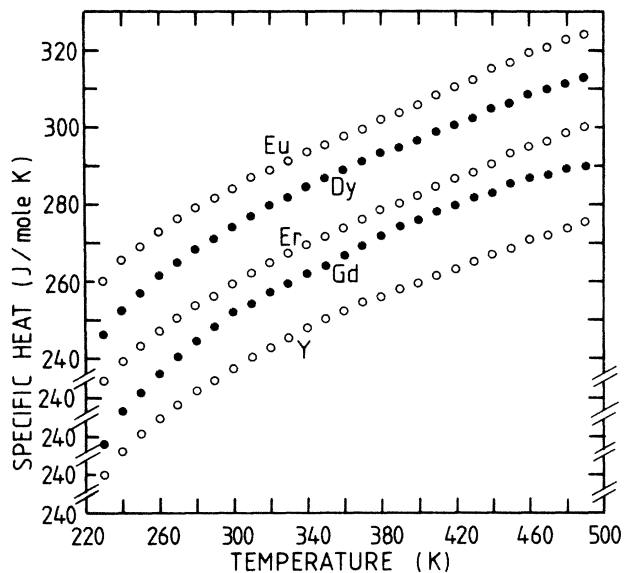


FIG. 6. Molar specific heat of five samples as a function of temperature in the range 230–490 K. Note that the vertical axis for each sample has been displaced for clarity.

ber of ions per mole. The ratio $C_{00}/3n_i k_B$ is about 1.4, implying that the Debye function accounts for approximately 70% of the total specific heat. We speculate that the remaining 30% of the specific heat measured in this temperature range could be related to spin waves, optical phonons, or stretching and bending modes of the copper-oxygen chains.

DISCUSSION

As mentioned above, the linear temperature dependence of the resistivity is suggestive of scattering of charge carriers by phonons. On the other hand, the temperature independence of the lattice thermal conductivity above the transition temperature can really be understood if the phonons are scattered mainly by electrons. To see why this is so, we use the simple formula given by Ziman⁷ which relates the lattice thermal conductivity to the electrical resistance due to phonon scattering:

$$\kappa_p \rho_{e-ph}/T = (k_B/e)^2 (n_0)^{-2} .$$

TABLE II. Specific heat of $\text{R}\text{Ba}_2\text{Cu}_3\text{O}_7$. C_{00} is the high-temperature limit from a fit to the Debye function, and $3n_i k_B$ is the theoretical Dulong-Petit value. C_p is the measured specific heat at 300 K.

R	Atomic weight, R (amu)	Molecular weight (amu)	$C_{00}/3n_i k_B$	C_p ($\text{J mol}^{-1} \text{K}^{-1}$)
Y	88.9	666.0	1.35	277.5
Eu	152.0	729.1	1.37	284.1
Gd	157.3	734.4	1.38	282.2
Dy	162.5	739.6	1.38	284.3
Er	167.3	744.4	1.36	279.3

Here n_0 is the number of electrons per unit cell. Using $\rho_{e-ph} = BT$, this becomes simply

$$\kappa_p = k_B^2 / (e^2 n_0^2 B) ,$$

which is constant, in good agreement with the experimental observation for $T > T_c$. Using the measured values of the thermal conductivity above the transition temperature and the parameter B given in Table I yields values for n_0 for each sample. These are presented in Table III. From the density and atomic weight of each compound we deduce the electron density, which, as shown in Table III, is in the range $(0.4-1.3) \times 10^{21} \text{ cm}^{-3}$. This compares favorably with Hall-effect data on La-Sr-Cu-O,⁸ and is small compared to normal metallic materials. The excellent fit of κ_p and ρ is the basis for our argument that electron-phonon interactions are very important.

Accepting, then, that the lattice thermal conductivity in the normal state is limited by carrier scattering, it is easy to understand the sharp increase of the thermal conductivity below the critical temperature. Electrons (or holes) which have become bound into Cooper pairs are no longer allowed to exchange energy with lattice vibrations. The lattice conduction therefore rises as more and more electrons are removed from the "normal" electron gas. Such behavior has been observed in lead alloys.^{9,10}

From our estimate for the carrier density and the phonon-limited resistivity ρ_{e-ph} , we can estimate the electron-phonon scattering time. We have

$$(\rho_{e-ph})^{-1} = ne^2 \tau_{e-ph} / m^* ,$$

where τ_{e-ph} is the electron-phonon scattering time and m^* the electron effective mass. Taking m^* as equal to free-electron mass and the values of n deduced above, this yields the values of τ_{e-ph} given in Table III, as well as the phonon-limited mobility $\mu_{e-ph} = e\tau_{e-ph}/m^*$. We see that the electron-phonon scattering time is very short, indicative of strong coupling between the two systems. Lead, for instance, which has a "high" critical temperature of 7.2 K, has an electron-phonon scattering time of about 10^{-12} s. Thus it appears that, if the superconductivity in the oxide compounds is indeed mediated by phonons, it is not a standard BCS system but a strongly coupled one. While these extremely short electron scattering times are incompatible within the framework of effective mass and relaxa-

tion time, our argument for electron-phonon coupling is not based on the Boltzmann equation, but on the relation between κ_p and ρ , which is essentially a count of the number of electron-phonon collisions.

In fact, we can estimate the size of the electron-phonon coupling constant from the scattering time. The lowest-order variational solution of the Bloch-Boltzmann transport equation yields¹¹

$$\hbar / \tau_{e-ph} = 2\pi \lambda_{e-ph} k_B T ,$$

where λ_{e-ph} is the electron-phonon coupling constant. From our deduced scattering times, we calculate λ_{e-ph} for each sample (Table III). Since $\lambda_{e-ph} > 1$, we are in the strong-coupling limit. In this case, the critical temperature is given approximately by¹²

$$T_c \sim \Theta_D \exp[-(1 + \lambda_{e-ph}) / (\lambda_{e-ph} - \mu^*)] ,$$

where Θ_D is the Debye temperature and μ^* is a dimensionless number which characterizes the strength of electron-electron interactions. It is given by¹²

$$\mu^* = V_c N_0 / [1 + V_c N_0 \ln(E_F / k_B \Theta_D)] ,$$

where N_0 is the density of electron states on the Fermi surface and V_c the matrix element of the Coulomb interaction. We have no knowledge of any information on the size of μ^* . We note, however, that, in the free-electron approximation, $E_F = 0.2-0.4$ eV for our samples, and $k_B \Theta_D = 0.04$ eV; thus, $\ln(E_F / k_B \Theta_D) > 1$ even in our sample with the lowest carrier density, and μ^* never exceeds 1. To gain a rough estimate of T_c , we use our values of λ_{e-ph} and Θ_D , and allow μ^* to vary between its extreme values of 0 and 1. This produces the range of critical temperatures given in Table III. Clearly, the measured Debye temperatures and the electron-phonon coupling constant as deduced from our data are large enough to produce a critical temperature in the range of that observed, regardless of the value assigned to μ^* . Even if, as has been suggested¹³ from a comparison of the magnetic susceptibility and the specific heat, m^* is five times the free-electron mass, values of T_c up to 100 K can be obtained. This lends support to a strongly coupled electron-phonon-mediated superconductivity in these compounds.

We return now to Fig. 5 and a discussion of the thermal conductivity below 6 K. As mentioned earlier, we find

TABLE III. Calculated parameters for $R\text{Ba}_2\text{Cu}_3\text{O}_7$. κ_c is the estimated carrier thermal conductivity at 100 K, n_0 is the number of electrons per unit cell, n is the number density of electrons, τ_{e-ph} is the electron-phonon scattering time, μ_{e-ph} is the phonon-limited electron mobility, λ_{e-ph} is the dimensionless electron-phonon coupling constant, and Θ_D is the Debye temperature from a fit to the specific heat.

R	x	y	κ_c ($\text{W cm}^{-1} \text{K}^{-1}$)	n_0	n (10^{21} cm^{-3})	τ_{e-ph} (10^{-15} s)	μ_{e-ph} ($\text{cm}^2 \text{V}^{-1} \text{s}^{-1}$)	λ_{e-ph}	Θ_D (K)	T_c (calc) (K)
Gd	1.98	3.05	0.00064	0.42	1.3	3	6	4.0	614	116-176
Dy	1.97	3.06	0.00058	0.34	1.2	4	7	3.0	595	81-157
Eu	1.93	2.92	0.00033	0.34	1.0	5	9	2.4	595	52-144
Y	2.01	3.11	0.00024	0.17	0.4	2	4	6.0	606	149-187
Er	2.03	3.05	0.00016	0.23	0.6	2	4	6.0	614	151-189

that in this temperature range $\kappa \sim T^3$. The simple kinetic formula

$$\kappa_p = c_p v L$$

relates the phonon thermal conductivity to the phonon specific heat c_p , the phonon velocity v , and the phonon mean free path L . Since the specific heat for $\text{YBa}_2\text{Cu}_3\text{O}_7$ has been observed to be cubic in temperature in this temperature range,¹⁴ the cubic dependence of κ_p suggests that the mean free path L of the phonons has become constant. It is natural, therefore, to suggest that at low temperature phonons scatter from the boundaries of the pores present in the crystal. In the case of a constant phonon mean free path, the lattice thermal conductivity is given approximately by¹⁵

$$\kappa_p = (2\pi^2 k_B^4 L / 15 \hbar^3 v^2) T^3.$$

If the phonon wavelength is less than the pore diameter d , and specular reflection of phonons at the surfaces is assumed, the mean free path is given by¹⁶

$$L = 0.59d/r.$$

Thus the lattice thermal conductivity is given by the expression

$$\kappa_p = (1.19\pi^2 k_B^4 d / 15 \hbar^3 v^2 r) T^3.$$

We can fit this expression to our data using d as an adjustable parameter. From the measured value of the porosity r and phonon velocities as given by Migliori, Chen, Alavi, and Gruener,¹⁷ we find for our sample $d \sim 5000 \text{ \AA}$. This compares well with the average pore diameter as observed with a scanning electron microscope (see Fig. 7). We note that the magnitude of our thermal conductivity is less than that measured by other workers.^{5,18} This we believe to be due to the smaller grain size and higher porosity of our samples. The porosity affects the thermal conductivity in two ways: First, it provides internal boundaries from which phonons can scatter (this is, in fact, the effect we have just discussed); and second, it reduces the effective cross section for transport. Zaitlin and Anderson¹⁶ have shown that for porosities in the range of those found in our



FIG. 7. Scanning electron micrograph of a portion of an $\text{YBa}_2\text{Cu}_3\text{O}_7$ sample. Hash mark indicates $0.1 \mu\text{m}$.

samples, the thermal conductivity can be reduced by as much as a factor of 4. We believe that this effect can account, to a large degree, for the discrepancy of results for different groups. Another possible reason for the difference in magnitude of κ for different groups is the composition of the sample. In Fig. 8, we show results of thermal conductivity measurements on three samples of different phase: a sample of $\text{YBa}_2\text{Cu}_3\text{O}_7$ of almost perfect 1:2:3 phase, a nonsuperconducting sample, and a superconducting sample which is rich in CuO. We see that this last sample has almost an order of magnitude higher thermal conductivity than the 1:2:3 sample, and also shows a smaller anomaly at the transition temperature. We believe this is due to the fact that the superconducting phase, which is responsible for the anomaly at T_c , occupies a smaller volume fraction in this sample, and the thermal conductivity is enhanced by the copper-rich phase which also reduces the porosity and provides better thermal contact between the grains.

CONCLUSIONS

We have measured the electrical resistivity, thermal conductivity, and specific heat of a series of high-temperature superconductors of the form $\text{RBA}_2\text{Cu}_3\text{O}_7$, with $R = \text{Y, Eu, Dy, Er, and Gd}$. The porous nature of the material affects both the electrical resistivity and the thermal conductivity. The electrical resistivity has a large temperature-independent component associated with scattering of charge carriers by pores, and a small linear component due to phonon scattering. The thermal conductivity is due almost entirely to lattice vibrations, and at high

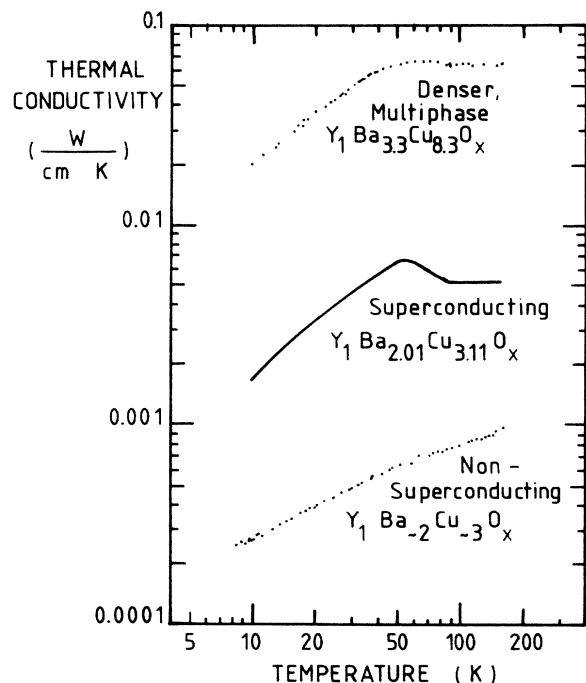


FIG. 8. Thermal conductivity of three different phases of Y-Ba-Cu-O .

temperatures is limited by carrier scattering. A sharp increase in κ_p below the critical temperature is attributed to the elimination of phonon-electron scattering in the superconducting state. The electron-phonon scattering time calculated from the thermal conductivity and electrical resistivity is on the order of 10^{-15} s, implying strong coupling between the two systems. Electron-phonon coupling constants deduced from this scattering time together with Debye temperatures derived from a fit to our specific-heat data are used to calculate the expected transition temperatures based on BCS theory in the strong-coupling limit. The resulting critical temperatures so deduced are in the range of those observed of all compounds. This, in and of itself, lends strong support to, but does not strictly imply,

BCS-type superconductivity in these compounds. The thermal conductivity at low temperatures (< 6 K) is limited by phonon-pore scattering, and an estimate of the pore diameter correlates well with that observed in scanning electron microscopy measurements.

ACKNOWLEDGMENTS

We gratefully acknowledge Charles Olk for assisting with the measurements, Jan Herbst for a critical reading of the manuscript, Bob R. Powell for discussions, and Noel Potter and Jack Johnson for carrying out chemical an x-ray analyses, respectively.

*Present address: Physics Department, University of Illinois, Champaign, Illinois 61801.

¹L. C. Bourne, A. Zettl, T. W. Barbee III, and M. L. Cohen, *Phys. Rev. B* **36**, 3990 (1987).

²M. Gurvitch and A. T. Fiory, *Phys. Rev. Lett.* **59**, 1337 (1987).

³K. J. Leary, H-C. zur Loye, S. W. Keller, T. A. Faltens, W. K. Ham, J. N. Michaels, and A. M. Stacy, *Phys. Rev. Lett.* **59**, 1236 (1987).

⁴D. T. Morelli, J. Heremans, and D. E. Swets, *Phys. Rev. B* **36**, 3917 (1987).

⁵V. Bayot, F. Delannay, C. Dewitte, J-P. Erauw, X. Gonze, J-P. Issi, A. Jonas, M. Kinany-Alauoi, M. Lambricht, J-P. Michenaud, J-P. Minet, and L. Piraux, *Solid State Commun.* **63**, 983 (1987).

⁶J. F. Herbst, using neutron data of W. I. F. David *et al.*, *Nature* **327**, 310 (1987).

⁷J. M. Ziman, *Electrons and Phonons* (Clarendon, Oxford, 1960).

⁸N. P. Ong, Z. Z. Wang, J. Clayhold, J. M. Tarascon, L. H.

Greene, and W. R. McKinnon, *Phys. Rev. B* **35**, 8807 (1987).

⁹J. L. Olsen, *Proc. Phys. Soc. London Sect. A* **65**, 518 (1952).

¹⁰P. Lindenfeld, *Phys. Rev. Lett.* **6**, 613 (1961).

¹¹F. J. Pinski, P. B. Allen, and W. H. Butler, *Phys. Rev. B* **23**, 5080 (1981).

¹²S. V. Vonsovsky, Yu.A. Izyumov, and E. Z. Kurmaev, *Superconductivity of Transition Metals* (Springer, Berlin, 1982); W. L. McMillan, *Phys. Rev.* **167**, 331 (1968).

¹³R. L. Green (private communication).

¹⁴M. E. Reeves, D. Citrin, B. G. Pazol, T. A. Friedmann, and D. M. Ginsberg (unpublished).

¹⁵R. Berman and J. C. F. Brock, *Proc. R. Soc. Ser. A* **289**, 46 (1965).

¹⁶M. P. Zaitlin and A. C. Anderson, *Phys. Rev. B* **12**, 4475 (1975).

¹⁷A. Migliori, T. Chen, B. Alavi, and G. Gruener, *Solid State Commun.* **63**, 827 (1987).

¹⁸J. J. Freeman, T. A. Friedmann, D. M. Ginsberg, J. Chen, and A. Zangvil (unpublished).

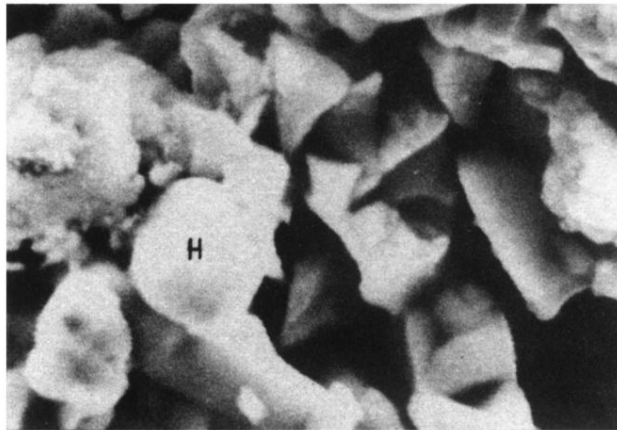


FIG. 7. Scanning electron micrograph of a portion of an $\text{YBa}_2\text{Cu}_3\text{O}_7$ sample. Hash mark indicates $0.1 \mu\text{m}$.